Received: 1 November 2018 | Revised: 7 January 2020 | Accepted: 17 January 2020

DOI: 10.1002/stc.2520

RESEARCH ARTICLE

WILEY

Damage detection for wind turbine rotor blades using airborne sound

Thomas Krause | **Jörn Ostermann**

Institut für Informationsverarbeitung, Leibniz Universität Hannover, Hannover, Germany

Correspondence
Thomas Krause, Institut für Informationsverarbeitung, Leibniz Universität Hannover, Appelstr. 9a, 30167 Hannover, Niedersachsen, Germany.
Email: krause@tnt.uni-hannover.de

Funding information
Bundesministerium für Wirtschaft und Energie, Grant/Award Number: 0324157A

Summary

When operating a wind turbine, damage of rotor blades is a serious problem. Undetected damages are likely to increase overtime, and therefore, the safety risks and economical burdens also increase. A monitoring system, which detects reliably defects in early stages, gives scope for action and is therefore a key element to avoid damage increase and to optimize the efficiency of wind turbines. One promising approach for damage detection is acoustic emission methods. Although most acoustic emission approaches use ultrasonic sound waves of the structure that require about 12 to 40 sensors to monitor one rotor blade, we propose to use the airborne sound in lower frequencies from about 500 Hz to 35 Hz with three optical microphones and present a signal model-based damage detection algorithm. The real-time algorithm uses six audio features from a spectrogram representation to detect damages and to estimate its significance. In a fatigue test of a 34-m blade, the algorithm detected the damage event and damage increasing without false detection. It was also tested with recordings inside an operating blade of a 3.4-MW wind turbine. In the recorded time period of about 1 year, the algorithm indicated no false detection.

KEYWORDS

acoustic emission, acoustic signal processing, airborne sound, damage detection, rotor blades, wind energy

1 | INTRODUCTION

Increasing the efficiency and safety of wind turbines is one important design goal that leads to many different research activities. Here, unexpected rotor blade damage is one important problem. In[1] the relevance of rotor blade damage for operating, a wind turbine is shown. Regular sight inspections of the blades are therefore mandatory. Nevertheless, these inspections cannot provide an instant damage detection, and even relatively small damages can accumulate overtime and lead to structural relevant damage. Besides the safety risk of an undetected damage, the economical burden increases rapidly if the damage increases, given the costs of repairs, replacement, and downtime.

There are many factors that prevent to solve this problem from the blade construction and production side. One aspect is the long lifespan in which extreme weather can occur. Another aspect is the need of lightweight blades and cost efficient production. The manual production of the large structure brings a margin of tolerance and makes it hard to guarantee a healthy lifetime of a rotor blade. All in all, it is unlikely that rotor blade damage can be eliminated from the construction and production side in the near future.

Monitoring the rotor blades is an approach to ease the problem. A system that detects rotor blade damages reliably and in early stages gives much better scope for action, and damage increase can be avoided. An ideal structural health monitoring (SHM) system also gives useful information of the damage, like the damage relevance. With such information, the efficiency of the wind turbine can be optimized by reducing the downtime and minimizing the cost of maintenance, repairs, and replacement. Thinking one step further, a system that predicts the remaining lifetime of a blade using the monitoring data opens up the possibility to optimize the overall economical benefits of the wind turbine with respect to the rotor blades.

Taking a look at the state-of-the-art of rotor blade SHM, one sees that quite a lot of research has to be done to achieve these goals. There are a few SHM systems on the marked. In the field of research, a variety of different damage detection approaches with the goal to provide a better performance exist.[2-4] One promising approach is based on acoustic emission event detection commonly referred to as acoustic emission (AE). Damage causes sound waves that are emitted in the structure and directly or indirectly into the air. The structural sound wave can be detected by monitoring physical values like the acceleration of the surface of the material. Sensors are often called AE sensors even if AE is not a physical quantity. This method was first prominently used to detect damages in a variety of different metal structures.[5] It was then transferred to damage detection of wind turbine blades, and plenty research was done under laboratory conditions, for example,.[6-8] For this method, ultrasonic frequencies are utilized; therefore, the amount of sensors is relatively high due to the size of modern blades and high internal damping of composite materials at these frequencies.[6,9] For monitoring, the whole rotor blade at least about one sensor every 2 m of the blade length is needed, which leads to many sensors given the length of 50 to 90 m of modern blades.

Rotor blades are complex structures made of a variety of materials, so there are a lot of different damage scenarios. In[10] seven different damage types, including combinations of delamination, fibre cracks debonding and so on were categorized suitable for the rotor blade context. Even within these categories, there are many possible scenarios how and where such damages happen, and what significance they have. In SHM research, it is a big challenge to design an accurate early damage detection methods, which covers all damage scenarios. Looking at the integrity of the structure, one rule of thump, which is often applied to AE methods, is high energy events in a short time period are an indicator of an important damage.

Up to now, there were only very few results published of AE systems in an operating wind turbine.[11-13] No damage happened during the monitored time periods in these research projects, and it is uncertain how the results under laboratory conditions can be translated into the real operational conditions where different environmental noise and side conditions are present. All event detection systems are confronted with this obstacle, and it is really hard to overcome, since it is very expensive or unlikely to capture a damage event in a full-scale operating wind turbine blade. The higher risk of damage from lightning strikes caused by the electrical conductive wires is one additional problem for typical AE approaches in operating rotor blades.[13]

Another closely related approach to monitor rotor blade damages is vibration-based methods, for example,.[14,15] Here, the vibration of parts of the blade caused by any excitation like wind or artificial excitation in the lower frequency range is captured and analyzed. The typical frequency range is lower than about 100 Hz. The signals are monitored, and based on the changes of the vibration signal, a damage state should be detected. With such methods, the damage can be detected even after the occurrence. Compared to AE methods, the drawbacks are less sensitive damage detection performance and longer time gaps to get the detection decision.

In contrast to other AE or vibration approaches, we propose to detect AE events by using airborne sound instead of the structure sound.[16-18] The idea is based on the observation that audible cracking sounds occur during rotor blade tests.[9] Common AE methods capture high ultrasonic frequency bands, but damage events did not radiate much energy in this frequency range into the air. On the other hand are the very low frequencies that are overlaid by environmental sounds with high energy, so we use the frequencies range from about 500 Hz to 35 kHz. The aim is to lower the amount of sensors compared to common AE approaches, due to the higher emitted energy and lower damping over distance in this lower frequency bands. Compared to vibration approaches, smaller damages should be detected. Additionally, optical microphones, which do not increase the risk of lightning strike damage, can be used to capture the sound in the air. In the used frequency range, cracking sounds as well as environmental noise can be found. This issue is dealt with by placing the focus on the signal processing aspect of the damage detection task.

From this perspective, damage detection with given sensor signals is a pattern recognition task. The pattern that should be detected is the cracking sound of a damage. There are two main approaches to solve such a task. The first approach is a signal model-based detection algorithm, which is designed by using knowledge and assumptions and translate this into an algorithm. Machine learning is the second approach, which is very popular these days. The two approaches can also

be combined so that parts are model-based and parts are derived by machine learning. We use audio features that were chosen based on a signal model, and the classification decision is derived by a decision tree that is a machine learning approach. Techniques as support vector machines were not used since we didn't have enough and divers damage sounds. Artificial neural networks that process the plain audio data and provide very good results in other audio classification tasks like speech recognition weren't used since they need much more data to function.

Machine learning detection algorithm is derived by using a predefined general algorithm, which is specified by a training process. The success of the training is based on the quantity and quality of the previously collected data. Machine learning approaches like Random Forest, Support Vector Machine, or Convolutional Neural Networks will work much better if the training data cover all combinations of events and boundary conditions that can occur in the monitoring scenario. This is a problem for rotor blade damage detection, since it is infeasible to record a lot of damage events covering different rotor blades, positions of damages and sensors, damage types, and so on. The dataset of damage (i.e. positive) events is always very small. For machine learning approaches with such a low amount of positive training data, overfitting is a serious problem and can barely be avoided. With a model-based approach, an algorithm can be designed, which considers scenarios that are not covered by the database but are likely to occur. This is a good strategy to avoid overfitting. Therefore, we designed our damage detection algorithm by building a model of the damage signal.

The typical way of designing a signal model-based pattern recognition algorithm is by using the sensor signals from which features are calculated. In the feature space defined by multiple features, all possible damage events build a cluster that should provide no or only a minimal overlap with the clusters of all other sound events. In a next step, the features are given to a classifier that implements the decision bounds.

The typical AE approach for rotor blade monitoring is parameter-based AE,[2-4] which is a simple form of a model-based detection algorithm. One damage event is typically called a hit. The standard approach for detecting a hit is to use the raw or filtered absolute time amplitude signal of a sensor. This signal is compared to a threshold value. If the signal exceeds the threshold in a given time period, a hit is signalled. If a certain amount of hits per time interval occur, the interpretation is that a significant damage happened.[19] The assumption for such pattern recognition algorithms is that the sensor signals provide damage signals with a higher amplitude than all other sounds like environmental sound and noise. In scenarios where the damage signal is masked, the complexity of the signal model must increase in order to avoid false alarms. Therefore, the proposed cheaper airborne sound damage detection system will need more advanced signal processing.

The airborne sound approach uses audio features calculated from the spectrogram representation, which describe characteristics of rotor blade damage sounds and a decision tree as a detector. The damage detection task is therefore solved by using audio classification (detection) techniques. The damage detection algorithm was tested during a full-scale fatigue test in.[18] In[20] we presented a localization approach and showed that the origin of the high power cracking sounds is the structural relevant damage. In[21] results were published of a vibration-based damage detection approach during the same fatigue test. In[22] a combination of the vibration approach with our airborne sound damage detection algorithm[18] can be found. Given the good standalone performance, in this paper, we investigate only the improved airborne sound damage detection method. Compared to,[18] we propose to use all microphone signals jointly and a different feature set that takes the condition in an operating wind turbine with a larger variation of noise levels better into account. We introduce a gradient-based power and a gradient-based tonal feature. Furthermore, the classifier now uses jointly the features from all microphones. This helps to consider different boundary conditions, and therefore, it should provide a more robust detection performance.

In Section 2, the airborne sound damage detection algorithm is described, which uses six audio features and estimates the significance of the damage. Two versions of the algorithm are described. One which can be applied using only one microphone and a version where all three microphones are used jointly. Then the fatigue test of a 34-m rotor blade is presented in Section 3, and the measurements in an operating 3.4-MW wind turbine blade can be found in Section 4, followed by Section 5, where the results of the damage detection algorithm using the data from the fatigue test and operation are presented. Section 6 concludes the paper.

2 | ALGORITHM FOR ROTOR BLADE DAMAGE DETECTION USING AIRBORNE SOUND

A real-time operating damage detection algorithm was developed, which detects rotor blade damages based on airborne sound signals. The algorithm is based on observations that were also made in previous versions of the algorithm.[16-18]

The signals are continuously captured inside the rotor blade at different positions. After the damage detection step, the algorithm estimates the significance of the damage based on the assumption that more relevant damages emit higher

sound energy. This assumption is backed by a lot of publications dealing with AE energy and failure modes like.[23] The aim is to detect relevant damage since very small damages like the cracking of a single fiber are considered as structural irrelevant in the rotor blade context.

The detection algorithm is based on a signal model of the specific impulse-like signals that represent audible rotor blade damage sounds in airborne sound recordings. A similar model was first developed by us in[16] based on the audio recordings during a certification test of a 55-m wind turbine blade. Based on the spectrogram representation, which display the frequency and power of the signal overtime, the signal model was build. The detection algorithm uses specific audio features according to the observed properties in the spectrogram data and checks continuously if the features are within the bounds that describe such signals. A similar approach and related features were used to detect other impulse sounds, since other impulse sounds share several properties. Examples are algorithms for drum sound classification[24] or gunshot detection.[25] In Figure 1, a typical rotor blade cracking sound with relatively low environmental noise level is displayed. We had observed the following signal properties, which all rotor blade cracking sounds have in common:

1. The damage sounds are described by an impulse characterized by sudden energy increase. The amount of energy varies.
2. The increase happens over a wide frequency range, which often exceeds the human hearing threshold of high frequencies.
3. The frequency at which the maximal power occurs can vary.
4. From the frequency with maximal power, its power decrease is approximately exponential towards high frequencies.
5. The decay of the power overtime is relatively slow and dependent on the positions of damage and sensor and the geometry of the blade.

The damage detection algorithm is structured as follows. First, a spectrogram representation is calculated (Section 2.1). In a next step, six audio features are calculated (Section 2.2) and sent to a classifier. There are two versions of the algorithm: one simple classifier uses features from a single microphone signal and the second classifier which uses features from multiple microphone signals jointly. The differences are described in Sections 2.3 and 2.4. Multiple detections in a short time frame are combined to one detection. One important criterion was to use audio features and classification decisions, which makes sense from the perspective of the signal properties. They have to be relatively robust against overlaid environmental noise signals and robust against variation of the position of the damage and sensor. After the damage detection step, the damage significance is estimated using power features from all channels and a weighting term (Section 2.5). In Figure 2, the flow chart of the single channel algorithm can be found. The multiple channel algorithm is depicted in Figure 3. The steps of the algorithm are described in the followings subsections.

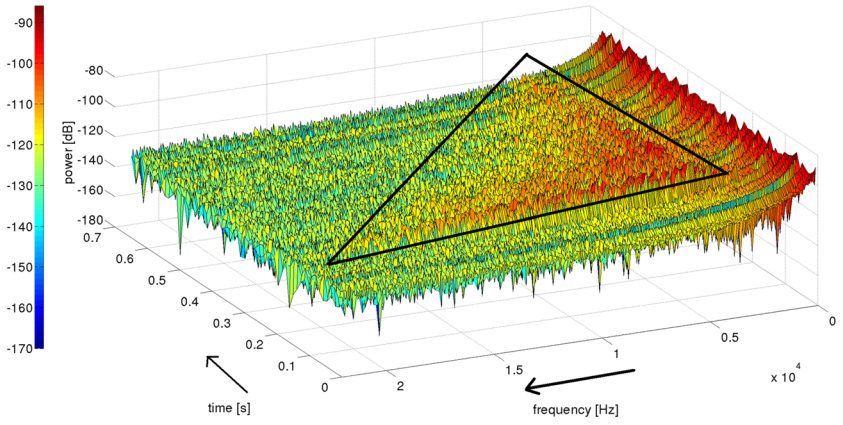

FIGURE 1 Spectrogram of a rotor blade cracking sound (marked area) with relatively low environmental noise. The power is also displayed in color

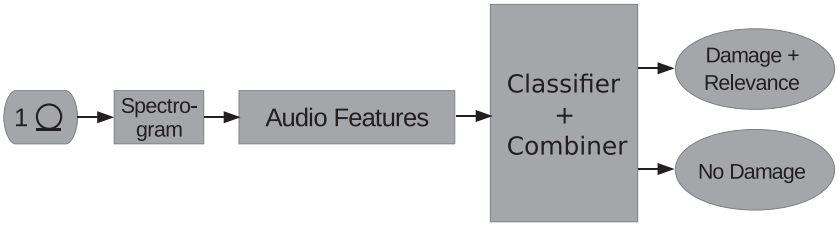

FIGURE 2 Principle flow chart of the damage detection algorithm using a single microphone

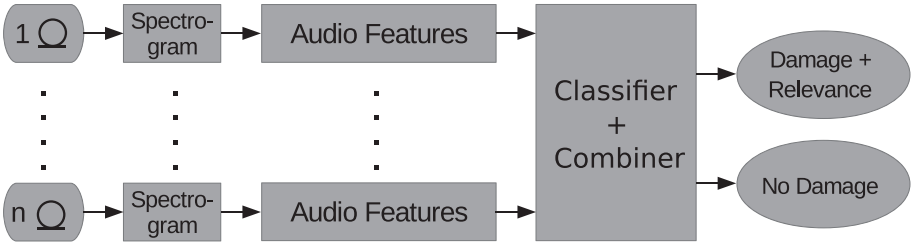

FIGURE 3 Principle flow chart of the damage detection algorithm using multiple microphones

2.1 | Spectrogram

In a first step, the audio data are transformed into a spectrogram representation. This is done continuously so that the further steps can use the spectrogram representation. For this, the discrete time amplitude signal $x(n)$ is transformed by a discrete short time Fourier transform where

$$S(k,l) = \sum_{n=0}^{N_{FT}-1} x\left(n + l \cdot \frac{N_{FT}}{2}\right) w(n) e^{-j\frac{2\pi nk}{N_{FT}}} \tag{1}$$

is performed. Here, l is the resulting time index and k the frequency index. A Hamming window $w(n)$ is used with the same length as the transformation length N_{FT}. The windows from two consecutive time indices l are half overlapped. The power spectrogram $P(k,l)$ is calculated using the squared absolute value and a normalization according to

$$P(k,l) = \frac{a}{N_{FT} \sum_{n=0}^{N_{FT}-1} |w(n)|^2} |S(k,l)|^2. \tag{2}$$

In the case of $k = 0$ or $k = N_{FT}/2$, the parameter a equals 1; in all other cases, a is 2. For the implementation of the algorithm, the transformation length $N_{FT} = 2048$ is used, which corresponds to about 20 ms and a frequency resolution of about 50 Hz at a sampling frequency of 96 kHz. With the half overlapping window, about every 10-ms new spectrogram data are available. The resulting spectrogram data are further processed to calculate characteristics of cracking sounds using the following six audio features.

2.2 | Audio features

The audio features are calculated by using two frequency ranges. The range from about 500 Hz to 35 kHz is used, since the environmental noise level in the frequencies below about 500 Hz is too high, and 35 kHz is the high frequency limit of the microphone. The second frequency range is from about 8 to 35 kHz. In this reduced frequency range, the power of the environmental noise signals is significantly lower. The downside is the higher reductions in power over distance especially if the sound has to travel around corners. Nonetheless, the reduced amount of environmental noise in this frequency range helps to provide more stable results for the detection and classification purpose, so it is used for five of the six features. The signal of a high power cracking sound has a significant amount of signal energy also above the hearing limit of about 20 kHz, and they can therefore be used for damage detection. We also tested a reduced highest frequency limit of 20 kHz instead of 35 kHz. Here, all time steps remain the same as the time steps in 96 kHz. The results can be found in Section 5. The features use different time periods, which are displayed in Figure 4. First, more important features are presented, which are used to remove many nondamage sounds, while the later features are used to check the details of a potential damage sounds. This order of the features is also used within the classifier in order to minimize compute resources.

2.2.1 | Power feature

Our assumption is that the damage relevance is increasing if the energy of the damage sound event increases, and only high power sounds indicate a relevant damage event. With this assumption, the first feature, which represents the power of the impulse, is calculated as follows:

$$f_1(l) = \sum_{k=k_{s1}}^{k_e} \sum_{l=l_{s1}}^{l_{e1}} P(k,l). \tag{3}$$

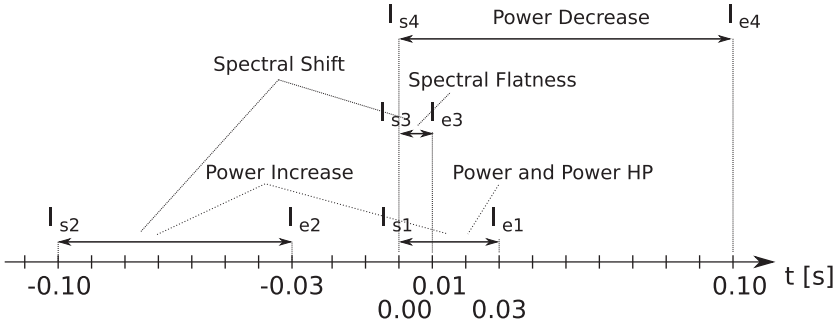

FIGURE 4 Discrete time bounds l of the six features illustrated in seconds. The Power and the Power HP feature use the time span from 0 to 0.03 s. The Power Increase feature uses the same time span and additionally the signal part from -0.1 to -0.03 s. The Spectral Flatness feature begins at 0 s and ends at 0.01 s. The Spectral Shift feature takes additionally the time frame from -0.1 to -0.03 s. The Power Decrease feature uses the time span from 0 to 0.1 s

Here, the spectrogram data from k_{s1} and l_{s1} to k_e and l_{e1} are summed up. The frequency range is set to 469 Hz to 35 kHz, and the time span is 32 ms.

2.2.2 | Power HP feature

In addition to the Power feature, the Power HP feature ensures that the sound contains significant energy in the higher frequencies. As mentioned before, there is less environmental noise present in this frequency bands. The feature is calculated as follows:

$$f_2(l) = \sum_{k=k_s}^{k_e} \sum_{l=l_{s1}}^{l_{e1}} P(k,l). \tag{4}$$

The time length is identical to the first power feature. The frequency range is from 7.96 to 35 kHz.

2.2.3 | Power increase feature

The third feature calculates the amount of power increase of the signal, which is used to detect the beginning of an impulse. Similar power gradient-based features are widely used for different audio classification tasks. Here, we used a modified power gradient feature that is calculated as follows:

$$f_3(l) = \frac{f_2(l)}{l_{e1} - l_{s1}} - \frac{\sum_{k=k_s}^{k_e} \sum_{l=l_{s2}}^{l_{e2}} P(k,l)}{l_{s2} - l_{e2}}. \tag{5}$$

The time indices l are also displayed in Figure 4. The time span of the subtrahend is longer than the time span of the minuend. This is done to get a better average of the noise power before the impulse. The gap between the two signal parts is used to take the attack time of the impulse into account.

2.2.4 | Spectral flatness

The spectral flatness measure[26] is calculated by dividing the geometric mean by the arithmetic mean of the power spectrum by

$$f_4(l) = \frac{\left(\prod_{k=k_s}^{k_e} P(k,l)\right)^{\frac{1}{k_e - k_s + 1}}}{\frac{\sum_{k=k_s}^{k_e} P(k,l)}{k_e - k_s + 1}}. \tag{6}$$

A value between zero and one is given, where zero represents a maximal tonal signal and one a maximal non-tonal signal. This measure was used for a lot of different audio detection and classification task, for example, to separate musical and percussive sounds.[27] The damage sounds, which are similar to percussive sounds, are non-tonal, but the power is exponentially decreasing towards higher frequencies, so this feature value should be closer to zero than to one.

2.2.5 | Spectral shift feature

This new feature is based on a logarithmic representation of the spectrogram in dB P_{dB}. From this representation, the spectral centroid is calculated by

$$s(l) = \frac{\sum_{k=k_s}^{k_e} F(k) \cdot P_{\mathrm{dB}}(k,l)}{\sum_{k=k_s}^{k_e} P_{\mathrm{dB}}(k,l)}, \tag{7}$$

Feature	Threshold	Upper or lower threshold	Threshold value	
			Sensitive	Insensitive
Power f_1	δ_1	lower	$3.6 \cdot 10^{-8}$	$1.0 \cdot 10^{-7}$
Power HP f_2	δ_2	lower	$2.3 \cdot 10^{-9}$	$1.2 \cdot 10^{-8}$
Power increase f_3	δ_3	lower	$1.2 \cdot 10^{-9}$	$1.1 \cdot 10^{-8}$
Spectral flatness f_4	δ_4	upper	0.54	0.31
Spectral shift f_5	δ_5	upper	−36	−110
Power decrease f_6	δ_6	upper	$-1.9 \cdot 10^{-11}$	$-1.6 \cdot 10^{-10}$

TABLE 1 Threshold values of the damage detection algorithm using a single microphone only

where F is a vector containing the center frequencies of all frequency bands. The spectral centroid represents the frequency, where the center of power is present and is used for similar audio detection tasks like gunshot detection.[25] In the next step, a slope of the spectral centroid signal is calculated by

$$f_5(l) = \frac{\sum_{l=l_{s3}}^{l_{e3}} s(l)}{l_{e3} - l_{s3}} - \frac{\sum_{l=l_{s2}}^{l_{e2}} s(l)}{l_{e2} - l_{s2}}. \tag{8}$$

Here, the time span of the subtrahend is also longer than the span of the minuend to get a better average of the sound component before the checked time span. With the assumption that the environmental noise is slower changing overtime than the damage sounds, the slope is robust against overlaid noise. We assume that the energy distribution of a damage sound is more geared towards lower frequencies than the energy distribution of environmental noise, so it can be used as an damage detection feature.

2.2.6 | Power decrease feature

The last feature evaluates the slope of the decrease in power overtime. Similar spectral slope features are also used for detection of the impulse-like sounds, for example, gunshot signals.[25] The power of the spectrogram in decibel is summed up by

$$p(l) = \sum_{k=k_s}^{k_e} P_{\,\mathrm{dB}}(k, l). \tag{9}$$

The frequency interval is from 7.96 to 35 kHz. Next, the slope of a simple linear regression function is calculated by

$$f_6(l) = \frac{\sum_{l=l_{s4}}^{l_{e4}} \left(l - \frac{\sum_{l=l_{s4}}^{l_{e4}} l}{l_{e4} - l_{s4}} \right) \cdot \left(p(l) - \frac{\sum_{l=l_{s4}}^{l_{e4}} p(l)}{l_{e4} - l_{s4}} \right)}{\sum_{l=l_{s4}}^{l_{e4}} \left(l - \frac{\sum_{l=l_{s4}}^{l_{e4}} l}{l_{e4} - l_{s4}} \right)^2}. \tag{10}$$

A time step equivalent of about 0.1 s is used with l_{s4} and l_{e4}. This covers the time span where the impulse power is approximately exponentially (linear in dB) decreasing overtime. We assume that in this interval, the amount of environmental noise is relatively low with respect to the power of the damage sound.

2.3 | Single channel classifier

First, a version of the algorithm with lower complexity that uses every microphone channel on its own to detect rotor blade damage is presented. The purpose of this classifier is to show the difference between single channel and multiple channel classification. All features described in the previous section are constantly calculated from the audio stream. The classification decision is made by a decision tree. A detection is derived if all six features satisfy the thresholds displayed in Table 1. The thresholds of the power features and power increase feature are dependent on the recording level, which is represented here with 0 $\mathrm{dB_{fs}}$ at 134 dB sound pressure level.

The thresholds were manually set to its values with regard of observed rotor blade cracking sounds and other impulse sounds like the cracking of branches and other impulse sounds which for the authors sound similar to actual rotor blade cracking sounds.

A relevant damage has to have high power in the low and high frequency range. Therefore, the power and power HP feature should be greater than δ_1 and δ_2, respectively. The power should be increasing over a short time period; therefore,

the power increase feature should be higher than the threshold δ_3. The damage signal power is exponentially decreasing towards higher frequencies, so the spectral flatness feature should be lower than the threshold δ_4. There should be a spectral shift of the spectral centroid towards lower frequencies; therefore, the spectral shift feature has to be lower than the threshold δ_5. The power of a damage sound is decreasing overtime, so the power decay feature should be lower than the threshold δ_6. If all features satisfy the thresholds, a detection is indicated. There are two parameter sets given which are called sensitive and insensitive, which should provide more detections with a higher risk of false positive detections or less detections, where true positive detections might be missed.

2.4 | Multiple channel classifier

The algorithm that detects rotor blade damage based on all microphone signals jointly is described in the following. It has the advantage of using the sound signal at different positions inside the rotor blade, which helps to make the detection decision more robust. Every microphone signal is affected by a different level and mixture of environmental noise and differences in the received damage sound due to the sound propagation paths. Therefore, features that use some kind of average over the positions should be more robust in comparison to a single channel detection strategy.

The multichannel features are constantly calculated from the audio streams and given to the multichannel decision tree where the features are compared threshold values. First, the six basic features described in Section 2.2 are calculated separately for every microphone signal. In the next step, these values were further processed to get the multichannel features d_{ij} and d_i.

Since the microphones have to be placed at different positions inside the rotor blade, and the damage can happen at any position, time differences of arrival of the recorded damage sounds will occur, which depend on the microphone positions. This is covered by an observation window that covers the time frame of the theoretical maximum time difference of arrival of the scenario. The time is simply calculated by dividing the speed of sound by the maximal sound path difference. The window defines how many feature values from the past are used for the damage detection step.

The features d_{ij} are used to check every channel on its own and are calculated by

$$d_{ij} = \begin{cases} \max_{l \in w} f_{ij}(l) & \text{if } i \in \{1,2,3\} \\ \min_{l \in w} f_{ij}(l) & \text{if } i \in \{4,5,6\}. \end{cases} \tag{11}$$

Here, f is the feature value of the feature with the number i, j the microphone channel, and $\max_{l=w}$ the maximal value within the observation window w. In Table 2, all features can be found. With the use of d_{ij}, it is checked if at least a significant damage signal is present at all microphones, which a relevant damage should provide. An irrelevant damage with a low overall energy would only be observable at the nearest microphones. Therefore, the thresholds δ_i are not so tightly chosen such that sound events that have to travel a longer distance to a microphone are still detected. The corresponding thresholds are equal to the "sensitive" thresholds from the single channel classifier.

The features d_i that use all microphones jointly are calculated by

$$d_i = \begin{cases} \left(\sum_{j=1}^{c} \max_{l \in w} f_{ij}(l)\right)/c & \text{if } i \in \{1,2,3\} \\ \left(\sum_{j=1}^{c} \min_{l \in w} f_{ij}(l)\right)/c & \text{if } i \in \{4,5,6\}. \end{cases} \tag{12}$$

TABLE 2 Overview of the threshold values of the damage detection algorithm using all microphones

Feature	Threshold	Upper or lower threshold	Threshold value
Power d_1	δ_{1m}	lower	$8.8 \cdot 10^{-8}$
Power d_{1j}	δ_1	lower	$3.6 \cdot 10^{-8}$
Power HP d_2	δ_{2m}	lower	$8.2 \cdot 10^{-9}$
Power HP d_{2j}	δ_2	lower	$2.3 \cdot 10^{-9}$
Power increase d_3	δ_{3m}	lower	$4.7 \cdot 10^{-9}$
Power increase d_{3j}	δ_3	lower	$1.2 \cdot 10^{-9}$
Spectral flatness d_4	δ_{4m}	upper	0.21
Spectral flatness d_{4j}	δ_4	upper	0.54
Spectral shift d_5	δ_{5m}	upper	−310
Spectral shift d_{5j}	δ_5	upper	−36
Power decrease d_6	δ_{6m}	upper	$-7.9 \cdot 10^{-11}$
Power decrease d_{6j}	δ_6	upper	$-1.9 \cdot 10^{-11}$

The features f in every channel are summed up and divided by the number of microphones c. The features d_i are used to check all microphone signals jointly. The thresholds δ_{im} for the features d_i are chosen more tightly than the threshold δ_i. Nevertheless, the features d_{ij} that check every signal channel are also needed, since it is possible that a small irrelevant damage sound occurs very close to one microphone, which provided a great value of d_i where only one microphone signal contributes to d_i.

The set of threshold parameters for the multiple channel classifier can be found in Table 2. Like for the single channel classifier, the thresholds of the power features and power increase feature are dependent on the representation of 0 dB_{fs}, which is here 134 dB_{spl}. All signals were normalized according to this. The detection decisions are

1. Power Feature: It is assumed that a relevant damage emits high signal power. The features values d_{1j} are checked if they are higher than the threshold δ_1 for all j microphone signals, and the feature d_1 is also checked if it is higher than the threshold δ_{1m}.
2. Power HP Feature: A relevant damage should also emit high signal power in the higher frequency range. Therefore, the values of the features d_{2j} should be higher than the threshold δ_2. The feature d_2 should also be greater than the threshold δ_{2m}.
3. Power Increase Feature: The third criteria test if there is a sufficient increase in power, which indicates the beginning of an impulse signal. The values of the features d_{3j} should be higher than the threshold δ_3. The feature d_3 should also be greater than the threshold δ_{3m}
4. Spectral Flatness: The impulse sound is exponentially increasing towards higher frequencies, which results in a lower spectral flatness value. The features values d_{4j} are checked if they are lower than the threshold δ_4 for all j microphone signals. The feature d_4 should also be lower than the threshold δ_{4m}
5. Spectral Shift: Damage sounds shift the spectral centroid towards lower frequencies. Therefore, features values d_{5j} are checked if they are lower than the threshold δ_5 for all j microphone signals. The feature d_5 should also be lower than the threshold δ_{5m}
6. Power Decay: Damage sounds should provide a power decrease overtime. The value of the features d_{6j} should be lower than the threshold δ_6. The feature d_6 should also be lower than the threshold δ_{6m}

If all criteria are met, a damage event is indicated for this time step. If there is no time gap between two or more detections, these detections are combined to one detection. In Figures 2 and 3, this part is called combiner.

2.5 | Damage significance estimation

If a detection is indicated, the significance of the damage is estimated as follows: the feature value d_2 is used, which is the sum of the maximum Power HP features in the time window. This measure corresponds with the observed damage significance. As mentioned, the assumption is backed up by a lot of publications dealing with AE energy and failure modes like.[23] We also tried to use the feature d_1 that uses also the low frequency content of the damage sounds, but we did not get as good results. This might be due to the higher environmental noise level in this frequency range. We tried to normalize the value according to our observations in a fatigue test, which is described in Section 3. The value one is here, the lowest relevant damage which was observed. This normalization might be a starting point for further investigations.

3 | ROTOR BLADE FATIGUE TEST

A test campaign including an edgewise fatigue test with a 34-m rotor blade was performed. The fatigue test aims to simulate the long-time stress of the blade in a relatively short time period, since it is infeasible to provoke damage of an operating full-scale rotor blade in regards of costs and time consumption. In the fatigue test, the blade is mounted with the root in a test block, and force is induced over one load frame that is mounted at the blade (Figure 5). The blade is excited near its first eigenfrequency so that the stress is distributed over the whole blade. The procedure is similar to the fatigue test for blade certification, which is described in detail in.[28] One difference is the load that was increased step by step to provoke damage of the blade. The other difference is that at least one full visual inspection was done everyday. The coating of the blade at the trailing edge was removed before the test in order to have better inspection possibilities of this area. One challenge of a full-scale rotor blade test is finding all damages that occur within each test period. The reference method here is a visual inspection, which has limitations in reliability and accuracy. Especially, small damages can easily be overseen or occur in parts which can not be inspected. In our case, the coating additionally prevented an accurate outside inspection of other parts than the trailing edge.

For the inspection, we also used a thermal camera. With the camera, we easily found parts where more stress in the rotor blade occurred. However, they gave no obvious additional hints of damage locations.

3.1 | Measurement set-up

For our method, three optical microphones were installed inside the blade according to Figure 6. The microphones were mounted orthogonal on the spars of the blade. Damping spiders were used for lowering the influence of vibrations induced into the microphone. The directionality of all microphones is specified as omnidirectional. During the test, the audio data were recorded nonstop with 96-kHz sampling rate and 24 bit precision. To monitor the blade and for gaining additional measurement data, strain gauges, accelerometers in different frequency domains, and velocity sensors were used.

3.2 | Observations of the fatigue test

In Table 3, a summary of the fatigue test and all documented damages are shown. Here ,100 % load is the calculated load at which the blade should collapse given one million cycles. During the first part of the rotor blade test, a lot of insignificant damages occurred. These small damages were glue cracks of overflowed glue at the trailing edge, small delaminations, small cracks of the blade coating, small inner cracks, and small surface cracks of the first layers. Some small pieces of the matrix of the outer layers were detached. We assume that none of these damages were relevant for the integrity of the structure since the sizes were small-like delaminations with a surface less than 8 cm^2, and the other characteristics of the damages also indicate a low significance, for example, cracks were only present in the first one or two layers of parts with many layers. The only structural relevant damage occurred at the second run with 170% load. The damage can be assigned to a narrow time span. Two consecutive loud cracking sounds occurred during the test Step 11b as well as a sudden decrease at some of the strain gauges that were used to monitor the test, and the test was stopped immediately. The crack was located at the length of about 6.25 m measured from the root of the blade. The continuous crack was present in all layers of the trailing edge and affected therefore the suction and pressure side. The crack length was at the beginning about 44 cm on both sides. There was a crack side arm on the pressure side that did not affect all layers. It had a length of about 7 cm. Since there was a visual inspection before and after test Step 11b, there are two possible scenarios for what happened. First, the whole damage occurred during the event, which leads to stopping the test, or second, a damage, which occurred earlier, was greatly increased within this event. According to the results of our damage detection system, this second scenario is much more likely. The fatigue test was continued with lower load to increase the crack. At the end of the fatigue test, the length of crack propagation in total was about 29.1 cm (adding the crack propagation of the three crack arms).

The three microphone signals were manually labelled. All cracking sounds were marked by the time of occurrence and by the number of microphones where the signals can be found. There are seven damage sounds with high sound pressure levels in all three microphone signals. There are two sounds in test Step 11b before the relevant damage. The cause of these events is likely an early damage stage of the continuous crack of the trailing edge. Two consecutive cracking sounds that have the highest power of all damage sounds can be associated with the occurrence of the continuous crack. All sounds

FIGURE 5 Picture of the rotor blade fatigue test that was conducted at Fraunhofer Institute for Wind Energy and Energy System Technology

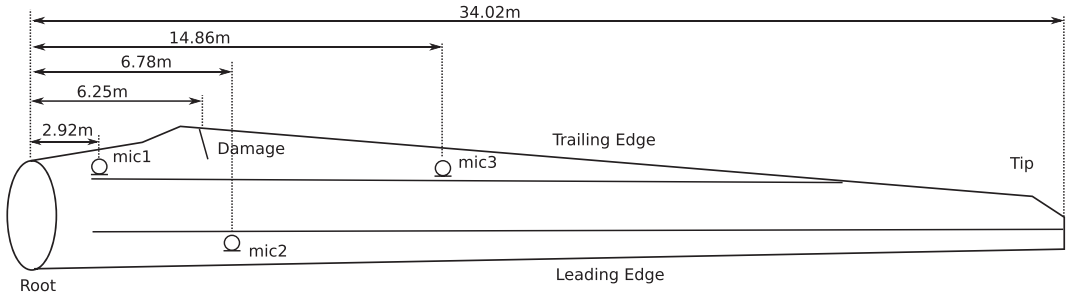

FIGURE 6 Principle drawing of the rotor blade measurements set-up of the fatigue test. At 6.25 m, the trailing edge crack occurred

TABLE 3 Overview of the fatigue test

Step	Load	Cycles	Visual inspection	Crack sounds high power	Crack sounds low power
1	70	94k	29 Insignificant damages	0	4
2	76	327k	20 Insignificant damages	0	0
3	81	94k	18 Insignificant damages	0	0
4	90	95k	28 Insignificant damages	0	0
5	96	103k	15 Insignificant damages	0	1
6	105	46k	2 Insignificant damages	0	1
7	110	278k	36 Insignificant damages	0	0
8	120	70k	36 Insignificant damages	0	4
9	130	13k	23 Insignificant damages	0	0
10	140	71k		0	3
11a	170	2k	6 Insignificant damages	0	133
11b	170	3k	Damage 44 cm	4	172
12	50	4k	Damage propagation	0	0
13	70	4k	0.3 cm	0	1
14	90	2k		0	0
15	105	10k	Damage propagation 8.9 cm	1	4
16	115	4k	Damage propagation 2.2 cm	0	0
17	130	4k	Damage propagation 17.7 cm	2	21

that occur after Step 11b are with high probability caused by crack propagation, since there were no other damages found in these time slots during the sight inspections.

There were also a lot of cracking sounds that have very low power and can only be found in one or two microphone signals. We tried to match these cracking sounds with the insignificant damages that were found during the visual inspection, but we did not find a valid relation between damages or damage types and the low power sound signals. In a few time slots, insignificant damages occurred near the microphone, and a cracking sound with lower power was found. But there were also cases where insignificant damage near a microphone occurred, but no cracking sound in the microphone data was found. More tests and research are needed to gain insides into the connection of very small damages and cracking sounds.

However, the signals with high power only occurred in test slots where relevant damage happened. In[20] we calculated the position of the sounds, and the localization results confirm the assumption that the source of all seven high power cracking sounds is the continuous crack. In addition, the differences in the three microphone signals in signal power and high frequency content also support the assumption. So these high power sounds are the target sounds to detect with the damage detection algorithm.

4 | MEASUREMENTS IN AN OPERATING WIND TURBINE BLADE

For testing the damage detection approach in a real-world scenario, we developed and installed a measuring system in an operating wind turbine. It was installed in one of the 50.8-m long rotor blades of a 3.4-MW class wind turbine. The turbine is located in Bremen, Germany.

4.1 | Measurement set-up of the operational measurements

The airborne sound measurements system consisted of three optical microphones that were installed inside the blade according to Figure 7. Here, the two microphones face the leading edge, since on this side, a greater distance between the microphones was feasible. The electric part of the measurement system was installed near the intersection of the hub and the root of the blade. The system consisted of a computer, electronic parts of the optical microphones, an audio interface, and an exchangeable storage. The audio data were recorded with 24 bit precision and 96-kHz sampling frequency. The files were losslessly coded with the flac audio codec. A global system for mobile device was used for controlling the system remotely.

4.2 | Observations of the operational measurements

We designed the measuring system for nonstop recording, since it is important to get data covering as many combinations of boundary conditions as possible. All in all, we managed to record about 1 year of audio signals. All weather events that typically occur in a year wise German seasonal cycle were recorded. These include heavy weather conditions like lightning, thunder, harsh wind, rain, hail, and snow. During the process of semi manually evaluation of the recordings, some events were found, which might be of interest like lightning strike sounds and one event which is a potential collision with a bird. No documented damage event occurred during the recording time period; therefore, the damage detection algorithm should indicate no detection.

5 | RESULTS OF THE DAMAGE DETECTION ALGORITHM

The recordings of the rotor blade fatigue test and the recordings from the operating wind turbine were both processed with the damage detection algorithm described in Section 2.

First, the results are presented for the algorithm that uses a single microphone channel to detect rotor blade damage. The two sets of parameters (sensitive and insensitive) from Table 1 were used to process the fatigue test data and the operational data. The results are displayed in Table 4. The overall performance when using one single microphone is not very convincing especially in the operational dataset. Here, plenty false positive detections were made. A lot of the false positive detections in the operational recordings occur in time periods where heavy rain was falling. The results of the damage detection of the fatigue test are significantly better, but the performance with some false positive and some missed detections is not very convincing either. In the fatigue test, most of the false alarms occur during test slots, with high load and therefore high operational noise.

In a following step, the algorithm that uses multiple microphone signals combined was tested. It was also tested with the whole dataset of the fatigue test and the whole operational dataset. We achieved very good results using all microphone

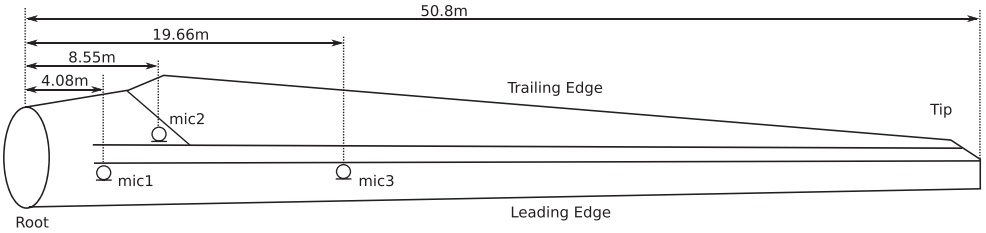

FIGURE 7 Principle drawing of the rotor blade measurements set-up in the operating rotor blade

TABLE 4 Results of the audio damage detection algorithm using a single microphone for the fatigue test and the operational dataset

	Fatigue		Operation	
	FP rate per day	TP rate	FP rate per day	TP rate
Microphone 1, sensitive	∼ 1,800	7/7	∼ 3,100	—
Microphone 2, sensitive	∼ 330	7/7	∼ 4,200	—
Microphone 3, sensitive	∼ 1,000	7/7	∼ 1,000	—
Microphone 1, insensitive	2.5	7/7	∼ 100	—
Microphone 2, insensitive.	0.1	2/7	∼ 400	—
Microphone 3, insensitive	1.7	4/7	∼ 35	—

Note. FP is the amount of false positive detections and TP rate the rate of true positive detections. The threshold parameter "sensitive" and "insensitive" from Table 1 are used.

signals combined. The thresholds from Table 2 are used. There is an adequate margin of all these parameters in which the results will not change, which indicates that this set of parameters might generalize. The results are shown in Table 5. The algorithm provides a perfect detection result detecting all damage sound events with no false alarms in both datasets. According to the evaluation of the fatigue test, the algorithm detects the continuous crack, two events that are likely the damage in an early stage and three events where the damage was increased. On the operational dataset, also no false detections were made. In Table 6 ,the amount of possible detections after every classification stage is shown for the fatigue test. A stage is here, one threshold decision according to the threshold of Table 2. Here, a detection indicates a damage event in a time slot of 10.7 ms. For Table 6, continuous detections were not grouped to single events.

We also tested a version of the algorithm where the maximum frequency of the input signal was reduced to 20 kHz instead of 35 kHz. The goal is to use the frequency range, which humans can perceive, and to evaluate the importance of the ultrasonic frequency band. The threshold values of the classifier were manually adjusted to the lower bandwidth of the signal. These thresholds can be found in the Appendix.

With the reduced frequency range, a perfect classification during the fatigue test was also achieved. In the recordings of the operating wind turbine, the algorithm provides one false positive detection. It was indicated in a part of the recording where heavy rain was falling and a thunder of a lightning strike occurred. The small theoretical benefits of using the extended frequency bandwidth can be shown here in the practical application, since it provides a perfect classification result during the fatigue test.

In the next step, the damage relevance was calculated. In Table 7, the estimated significance of all damage events is shown. There are not many damage events in the dataset, and additionally, the ground truth from the visual inspection was done after every fatigue test step,and therefore, not every single damage sound can be associated to a specific crack length. It is hard to say if the approach is in general valid, but nevertheless, the estimation shows good correspondence with the observed damage sizes of the visual inspections.

TABLE 5 Results of the audio damage detection algorithm using three microphones jointly for the fatigue test and the operational dataset

Fatigue		Operation	
False positive	**True positive rate**	**False positive**	**True positive rate**
0	7/7	0	-

TABLE 6 Number of detections after the classification stages for the fatigue test data (multiple detections are not combined here)

Stage	Number of raw detections
Before Cl.	$7.8 \cdot 10^7$
1	2,351,867
2	1,822,183
3	2,725
4	616
5	201
6	192
7	119
8	110
9	76
10	75
11	75
12	74

TABLE 7 Estimated damage relevance by the algorithm of the detected damage events

Event	Damage description	Damage length	Relevance value
1	55 min before damage	44 cm	1.26
2	1 min before damage		4.04
3	Structural damage		16.83
4	Structural damage		21.03
5	Damage propagation	8.9 cm	1.00
6	Damage propagation	17.7 cm	1.50
7	Damage propagation		0.09

Note. The damage length is not always associated to one single sound event due to the visual inspection.

6 | CONCLUSION

In this paper, an AE method using airborne sound for damage detection of wind turbine rotor blades was presented. The number of three sensors is significantly lower compared to standard AE approaches. The key aspect is the damage detection algorithm, which uses airborne AE in lower frequency bands below 35 kHz, and handles environmental noise, which is also present in this frequency range. Six audio features that represent characteristics of audible cracking sounds are calculated for three microphone signals. These features are jointly used to detect the damage sounds. The algorithm detects relevant damage events of a full-scale fatigue test without false detections. In the next step, the real-time operating algorithm estimates the significance of the detected damages with a good correspondence to the observed damage events. In 1 year data of an operational 3.4-MW wind turbine blade, the algorithm indicates no false detections.

Since it is very expensive and time consuming to get meaningful data for rotor blade damage detection, there is still a level of uncertainty on how this method will perform in different rotor blade monitoring scenarios. Nevertheless, the very good results will hopefully translate in future rotor blade monitoring research and applications. Furthermore, it indicates the general benefits of using the lower AE frequency range with signal processing techniques.

ACKNOWLEDGEMENTS

This research was funded by German Federal Ministry for Economic Affairs and Energy (BMWi) "Multivariate Structural Health Monitoring for Rotor Blades" (0324157A).

ORCID

Thomas Krause https://orcid.org/0000-0002-4304-7154

REFERENCES

1. Tavner P. Offshore wind turbines- reliability, availability and maintenance. The Institution of Engineering and Technology; 2012.
2. Ciang CC, Lee J-R, Bang H-J. Structural health monitoring for a wind turbine system: a review of damage detection methods. *Measuement Science and Technology*. 2008;19:122001.
3. Schubel PJ, Crossley RJ, Boateng EKG. Review of structural health and cure monitoring techniques for large wind turbine blades. *Renew Energy*. 2012;51:113-123.
4. Yang W, Tavner PJ, Crabtree CJ, Feng Y, Qiu Y. Wind turbine condition monitoring: technical and commercial challenges. *Wind Energy*. 2014;17(5):673-693.
5. McMaster RC. Nondestructive Testing Handbook; 1982.
6. Beattie AG. Acoustic emission monitoring of a wind turbine blade during a fatigue test. 35th Aerospace Sciences Meeting; 1997.
7. Kirikeraa GR, Shindea V, Schulza MJ, Ghoshal A, Sundaresan M, Allemang R. Damage localisation in composite and metallic structures using a structural neural system and simulated acoustic emissions. *Mech Syst Signal Process*. 2007;21:280-297.
8. Zarouchas D, Antoniou A, Sayer F, Van Hemelrijck D, van Wingerde A. Structural integrity assessment of blade's subcomponents using acoustic emission monitoring. In: T Proulx, ed. *Experimental and Applied Mechanics, volume 6*. New York, NY: Springer; 2011:511-518.
9. Sørensen BF, Lading L, Sendrup P, et al. Fundamentals for remote structural health monitoring of wind turbine blades-a preproject. Forskningscenter Risoe. Risoe-R, No. 1336(EN) 36 p; 2002.
10. Blanch MJ, Dutton AG. Acoustic emission monitoring of field tests of an operating wind turbine. *Key Eng Mater*. 2003;245-246:475-482.
11. Papasalouros D, Tsopelas N, Ladis I, et al. Health monitoring of a neg-micron nm48/750 wind turbine blade with acoustic emission; 2012.
12. Worms K, Klamouris C, Wegh F, et al. Reliable and lightning-safe monitoring of wind turbine rotor blades using optically powered sensors. *Wind Energy*. 2017;20(2):345-360.
13. Tsiapoki S, Häckell MW, Grießmann T, Rolfes R. Damage and ice detection on wind turbine rotor blades using a three-tier modular structural health monitoring framework. *Struct Health Monit*. 2018;17(5):1289-1312.
14. Oliveira G, Magalhães F, Cunha Á, Caetano E. Vibration-based damage detection in a wind turbine using 1 year of data. *Struct Control Health Monit*. 2018;25(11):e2238.
15. Krause T, Preihs S, Ostermann J. Detection of impulse-like airborne sound for damage identification in rotor blades of wind turbines. 7th European Workshop on Structural Health Monitoring (EWSHM2014); 2014a.
16. Krause T, Preihs S, Ostermann J. Airborne sound based damage detection for wind turbine rotor blades using impulse detection in frequency bands. In: 1st International Wind Engineering Conference (IWEC); 2014b.
17. Krause T, Preihs S, Ostermann J. Acoustic emission damage detection for wind turbine rotor blades using airborne sound. Proceedings of the 10th International Workshop on Structural Health Monitoring (IWSHM2015); 2015.
18. Joosse PA, Blanch MJ, Dutton AG, Kourousis D, Philippidis TP, Vionis PS. Acoustic emission monitoring of small wind turbine blades. *J solar energy eng*. 2002;124(4):446-454.
19. Grosse CU, Ohtsu M. *Acoustic Emission Testing*. Heidelberg: Springer Science & Business Media; 2008.

20. Krause T, Ostermann J. Acoustic emission localization using airborne sound: Where did the wind turbine rotor blade crack?. 9th European Workshop on Structural Health Monitoring (EWSHM2018); 2018.
21. Tsiapoki S, Häckell M, Rolfes R. Monitoring of a 35 m wind turbine rotor blade during a fatigue test by a modular shm-scheme. In: Proceedings of the 10th International Workshop on Structural Health Monitoring (IWSHM2015); 2015.
22. Tsiapoki S, Krause T, Häckell MW, Rolfes R, Ostermann J. Combining a vibration-based shm-scheme and an airborne sound approach for damage detection on wind turbine rotor blades. In: Proceedings of the 8th European Workshop on Structural Health Monitoring (EWSHM 2016); 2016.
23. Ono K. Acoustic emission behavior of flawed unidirectional carbon fiber-epoxy composites. *J Reinf Plast Compos*. 1988;7(1):90-105.
24. Herrera P, Yeterian A, Gouyon F. Automatic classification of drum sounds: a comparison of feature selection methods and classification techniques. In: C Anagnostopoulou, M Ferrand, A Smaill, eds. *Music and artificial intelligence*. Berlin, Heidelberg: Springer; 2002:69-80.
25. Valenzise G, Gerosa L, Tagliasacchi M, Antonacci F, Sarti A. Scream and gunshot detection and localization for audio-surveillance systems. In: Advanced Video and Signal Based Surveillance, 2007. avss 2007. ieee conference on IEEE; 2007:21-26.
26. Gray AH, Markel JD. A spectral-flatness measure for studying the autocorrelation method of linear prediction of speech analysis. *IEEE Trans Acoust Speech Signal Process*. 1974;22:207-217.
27. Canadas-Quesada F, Vera-Candeas P, Ruiz-Reyes N, Munoz-Montoro A, Bris-Penalver F. A method to separate musical percussive sounds using chroma spectral flatness. SIGNAL 2016 Editors 51; 2016.
28. IEC 61400-23 TS Ed.1. Wind turbine generator systems–part 23: full-scale structural testing of rotor blades. Edition 2001.

How to cite this article: Krause T, Ostermann J. Damage detection for wind turbine rotor blades using airborne sound. *Struct Control Health Monit*. 2020;27:e2520. https://doi.org/10.1002/stc.2520

APPENDIX A: THRESHOLDS MULTICHANNEL CLASSIFIER 20KHZ

The thresholds for the multichannel classifier from Section 2.4 were adjusted according to a reduced maximum frequency of the audio data. The maximum frequency of 20 kHz is chosen (34 kHz in Section 2.4), which is approximately the hearing threshold of humans. In Table A1, the multichannel classification thresholds are displayed.

TABLE A1 Overview of the threshold values of the damage detection algorithm using all microphones for the maximum frequency of the audio signal of 20 kHz

Feature	Threshold	Upper or lower threshold	Threshold value
d_1	δ_{1m}	lower	$7.4 \cdot 10^{-9}$
d_{1j}	δ_1	lower	$2.7 \cdot 10^{-9}$
d_2	δ_{2m}	lower	$9.2 \cdot 10^{-10}$
d_{2j}	δ_2	lower	$4.2 \cdot 10^{-10}$
d_3	δ_{3m}	lower	$7.8 \cdot 10^{-10}$
d_{3j}	δ_3	lower	$9.1 \cdot 10^{-11}$
d_4	δ_{4m}	upper	0.35
d_{4j}	δ_4	upper	0.55
d_5	δ_{5m}	upper	−14
d_{5j}	δ_5	upper	−5
d_6	δ_{6m}	upper	$-1.3 \cdot 10^{-10}$
d_{6j}	δ_6	upper	$-6.1 \cdot 10^{-12}$